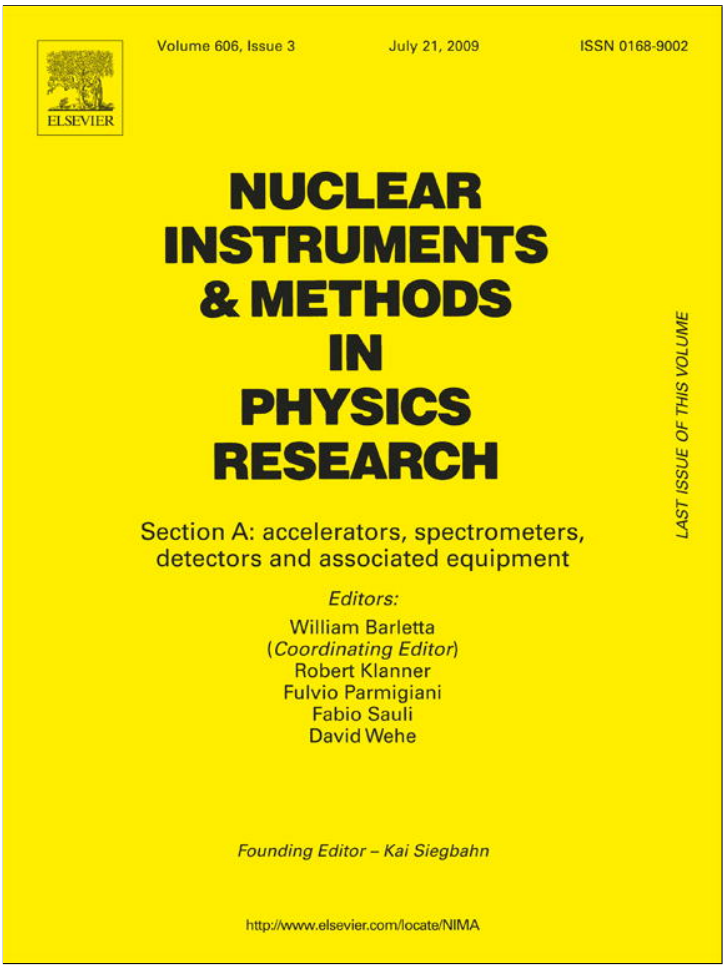

Nuclear Instruments and Methods in Physics Research A 606 (2009) 749–754

Contents lists available at ScienceDirect

Nuclear Instruments and Methods in Physics Research A

journal homepage: www.elsevier.com/locate/nima

Monte-Carlo based prediction of radiochromic film response for hadrontherapy dosimetry

T. Frisson [a,b,d,*], N. Zahra [a,c,d], P. Lautesse [a,c], D. Sarrut [a,b,d]

[a] Université de Lyon, F-69622 Lyon, France
[b] CREATIS-LRMN, INSA, Bâtiment Blaise Pascal, 7 avenue Jean Capelle, 69621 Villeurbanne Cedex, France
[c] IPNL - CNRS/IN2P3 UMR 5822, Université Lyon 1, Bâtiment Paul Dirac, 4 rue Enrico Fermi, F-69622 Villeurbanne Cedex, France
[d] Centre Léon Berrard - 28 rue Laennec, F-69373 Lyon Cedex 08, France

ARTICLE INFO

Article history:
Received 19 January 2009
Received in revised form
14 April 2009
Accepted 16 April 2009
Available online 3 May 2009

Keywords:
Radiochromic film
Dosimetry
Hadrontherapy
Monte-Carlo simulation
Linear energy transfer
Photon irradiation
Carbon irradiation

ABSTRACT

A model has been developed to calculate MD-55-V2 radiochromic film response to ion irradiation. This model is based on photon film response and film saturation by high local energy deposition computed by Monte-Carlo simulation. We have studied the response of the film to photon irradiation and we proposed a calculation method for hadron beams.

1. Introduction

For many years, films have been used in radiotherapy to determine dose distribution. The film response is well known for such classical applications. Hadrontherapy uses different beam types, which makes the film response more complex.

Radiochromic films seem to be useful detectors for dosimetry with hadron beams because of their high spatial resolution which allows to measure dose distributions in regions of high-dose gradient. The film resolution is better than 1 μm per pixel [1]. The MD-55-V2 radiochromic films studied in this work are 310 μm thick, with two 16 μm sensitive layers of diacetylene monomeric microcrystals on a clear polyester base. The sensitive layers undergo partial polymerization by the ionizing radiation [2]. The irradiated films have two absorption peaks in the red region of the spectrum centered at 614 and 674 nm [3] hence the film color is blue. These peaks increase as the absorbed dose increase and the films darken.

With the photon beam of a typical radiotherapy accelerator, film response is simply a function of the dose (see Section 2.1). However, with hadron beams, film response also depends on the hadron track structure i.e. hadron charge and energy, especially near the Bragg peak. For the same total dose to the film, local ionization and dose are much higher around ion tracks when using hadron beams, whereas they are more uniformly distributed over the whole film when using photons. Film response could become more complex with the fragmentation of the hadrons in the material which produces new particles of different atomic numbers and energies. Formation of a spread-out Bragg peak (superposition of several beams with different energies) also contributes to modifying film response when using hadron beams.

In this study, we propose a model to predict response as a function of the local behavior of the film irradiated using hadron beams. Film response to photon beams is used as a reference to calculate response to ion irradiation. We will first study the response of the film to photons, then propose a calculation method for ion beams.

2. Optical density

The MD-55-V2 film dose response can be calculated using the absorption spectrum of the film and the light spectrum of the scanner [4]. The present study aimed to establish the global behavior of the film as a function of the dose absorbed and of incident particle features. In particular, we studied the energy

* Corresponding author at: CREATIS-LRMN, INSA, Bâtiment Blaise Pascal, 7 avenue Jean Capelle, 69621 Villeurbanne Cedex, France.
E-mail address: frisson@creatis.insa-lyon.fr (T. Frisson).

0168-9002/$ - see front matter © 2009 Elsevier B.V. All rights reserved.
doi:10.1016/j.nima.2009.04.027

deposition close to the track. Indeed, the density of deposited energy around an ion track is very high and may influence film response. We defined the local linear energy transfer (local LET) as the energy deposited along a track segment in a cylinder of radius r centered on the track segment divided by the length of the track segment. We considered r to be smaller than the size of polymer microcrystals, i.e. in the order of the micrometer.

2.1. Low local LET particles

For particles with low local LET, the light transmittance through an infinitesimal surface area dS of a film irradiated to a dose D_{dS} is

$$T_{dS}(\lambda, D_{dS}) = \frac{I(\lambda, D_{dS})}{I_0(\lambda)} \tag{1}$$

where $I_0(\lambda)$ is the intensity of the light for the wavelength λ passing through the film and $I(\lambda, D_{dS})$ the intensity after the film. $I_0(\lambda)$ and $I(\lambda, D_S)$ are dependent on the light source of the scanner used to read the film. The optical density is defined as

$$OD_{dS}(D_{dS}) = -\log\left(\frac{\int_0^\infty I(\lambda, D_{dS})\, d\lambda}{\int_0^\infty I_0(\lambda)\, d\lambda}\right). \tag{2}$$

We consider that the optical density can be expressed with parameters a and b:

$$OD_{dS}(D_{dS}) = -\log\left(\frac{1}{I_0^{tot}(a \cdot D_{dS} + b)}\right) = \log(I_0^{tot}(a \cdot D_{dS} + b)) \tag{3}$$

where $T(0) = 1/(I_0^{tot} \cdot b)$ is the transmittance value of an unirradiated film and $I_0^{tot} = \int_0^\infty I_0(\lambda)\, d\lambda$ is the total intensity of the light. The net optical density is defined as

$$OD_{dS}^{net}(D_{dS}) = OD_{dS}(D_{dS}) - OD_{dS}(0) \tag{4}$$

$$OD_{dS}^{net}(D_{dS}) = \log(I_0^{tot}(a \cdot D_{dS} + b)) + \log(T(0)) \tag{5}$$

$$OD_{dS}^{net}(D_{dS}) = \log(a' \cdot D_{dS} + 1). \tag{6}$$

We consider that the light spectrum is stable over the whole scan area. For a surface S of the film irradiated to a dose D, the transmittance is

$$T(D) = \frac{1}{S}\int_S T_{dS}(D_{dS})\, dS = \frac{1}{S}\int_S \frac{1}{(I_0^{tot}(a \cdot D_{dS} + b))}\, dS. \tag{7}$$

The optical density is

$$OD(D) = -\log(T(D)) = -\log\left(\frac{1}{S}\int_S \frac{1}{(I_0^{tot}(a \cdot D_{dS} + b))}\, dS\right) \tag{8}$$

$$OD^{net}(D) = -\log\left(\frac{1}{S}\int_S \frac{1}{(a' \cdot D_{dS} + 1)}\, dS\right). \tag{9}$$

And for a homogeneous dose D over the whole surface S of the film:

$$OD^{net}(D) = OD_{dS}^{net}(D) = \log(a' \cdot D + 1). \tag{10}$$

2.2. High local LET particles

The track structure of heavy charged particles is characterized by high energy deposition along trajectories. The energy deposited may be locally higher than the film capabilities. This can be seen as a saturation of the film and the excess energy deposited is lost, i.e. does not contribute to darkening the film. The coloration of the film around the track is lower than the coloration of films irradiated homogenously at the same dose with low local LET particles. Accordingly, the coloration likely corresponds to an irradiation with low local LET particles delivered at a lower dose named effective dose, or D_{eff}. To model this behavior, we have looked for a function to express the effective local linear energy transfer LET_{eff} as the function of the local LET of the particle. At low local LET, the equation yields $LET_{eff} = LET$ and in the high local LET region, the function shows a saturation without horizontal asymptote. In the case of a homogeneous irradiation, the effective local linear energy transfer LET_{eff} is expressed as the function of the local LET of the particle:

$$LET_{eff} = \tau \ln\left(\frac{LET}{\tau} + 1\right) \tag{11}$$

where τ is the limit of the linear region of the film effective local LET. The effective dose deposited by a particle along a track segment L is

$$D_{eff} = \frac{LET_{eff} \cdot L}{M} \tag{12}$$

where M is the mass of the film volume considered. And the optical density is

$$OD^{net}(D_{eff}) = \log(a' \cdot D_{eff} + 1) \tag{13}$$

where a' is the film response parameters defined in the previous section. In cases where LET/τ tends toward zero:

$$LET_{eff} = \tau \ln\left(\frac{LET}{\tau} + 1\right) \to LET. \tag{14}$$

And, we retrieve Eq. (10)

$$OD^{net}(D_{eff}) \to OD^{net}(D). \tag{15}$$

3. Experimental setup and simulation

3.1. Experimental setup

In this study, we used Gafchromic® MD-55-V2 radiochromic films (International Specialty products, Wayne, NJ, batch # P0234MDV2). The films were read four days after irradiation using a Vidar VXR-16 DosimetryPRO Film Digitizer (Vidar Corporation, Herndon, Virginia) at the Centre Léon Berard (Lyon, France). This scanner has a fluorescent white light source with a spectral emission range between 250 and 750 nm. It is coupled to a linear CCD digitizing system. The resolution used was 89 μm per pixel. Films were taped onto transparency paper and scanned using the Omnipro IMRT software (Scanditronix Wellhofer). Optical density was measured with about 5% accuracy [1].

Photon irradiations were carried out at the Centre Léon Berard (Lyon, France) using an Elekta 6 MV beam linear accelerator with the films placed perpendicularly to the radiation beam. Ten centimeters of solid water was present before the film position. Films were irradiated at several doses between 0 and 150 Gy. To read the films, we chose a region of interest in the center of the film ($\simeq 1\,cm^2$) and we measured the dose at the film position with a thimble ionization chamber. The precision of dose measurements was 2% and the error on the dose delivered was less than 1%.

Ion irradiations were done at GANIL (Caen, France). A PMMA triangle (2 cm × 4 cm × 5 cm) was installed in front of a film and irradiated with a 75 MeV/u ^{13}C beam at 20 Gy and with a 95 MeV/u ^{12}C beam at 60 Gy (see Fig. 1). Using this experimental setup, we obtained the deposition of the whole Bragg curve in one film by measuring the optical density along the x axis. Note that the angle of the triangle allows to spread ($\alpha < 45^\circ$) or to shrink ($\alpha > 45^\circ$) the Bragg curve, whereas an angle of 45° conserves lengths. Experiments at the GANIL were performed using an α angle of 35°, so we had to apply a correction to the position. The correction

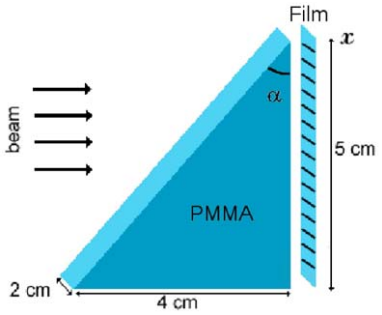

Fig. 1. Experimental setup for the experiment at the GANIL. A triangle of PMMA is installed in front of the film. Optical density is measured along the x axis to obtain the whole Bragg curve.

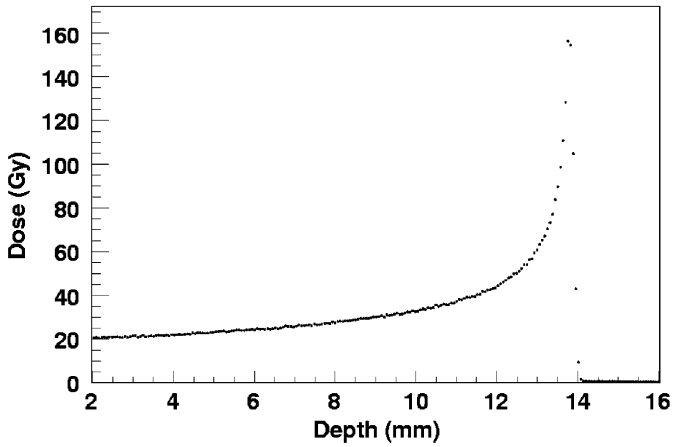

Fig. 2. Simulation of dose deposition in film as a function of the position along the x axis using a 75 MeV/u ^{13}C beam (see the GANIL experimental setup).

factor was $\tan\alpha = 0.7$. The precision was limited by the scanner resolution. The size of each bin was 89 μm. The GANIL accelerator consists of two separated sector room temperature cyclotrons which produce heavy ions from C to Ar with energy up to 95 MeV/u and can accelerate masses up to U at 25 MeV/u. The end of the beam line is closed by a 15 μm wide stainless steel sheet. We measured the dose at the phantom entry with a thimble ionization chamber and a plane parallel ionization chamber. The error in dose measurement was 2% and the error in the dose delivered was about 1%.

3.2. Simulation

Simulations were done with the GATE software based on Geant4 version 4.9.1 patch 02 [5,6]. The tools used in this study will be included into the next public release of the GATE software. We used the physics list named QGSP_BIC_HP with low energy models. All experimental conditions used for photon and ion irradiations, as described in the previous section, were taken into account in the simulation. The particle density used in the simulation was the same as in the experiment realized at the GANIL ($d = 1.95 \times 10^6$ particles/cm^2 for the ^{13}C beam and $d = 2.25 \times 10^6$ particles/cm^2 for the ^{12}C beam). Fig. 2 shows a simulation of the dose-depth profile as a function of the position corresponding to the ^{13}C beam experimental conditions. We verified that the dose deposition at the beginning of the simulated Bragg curve was identical to the dose measured with the ionization chamber ($\text{Dose}_{measure} - \text{Dose}_{simulation} = 0.37$ Gy). The

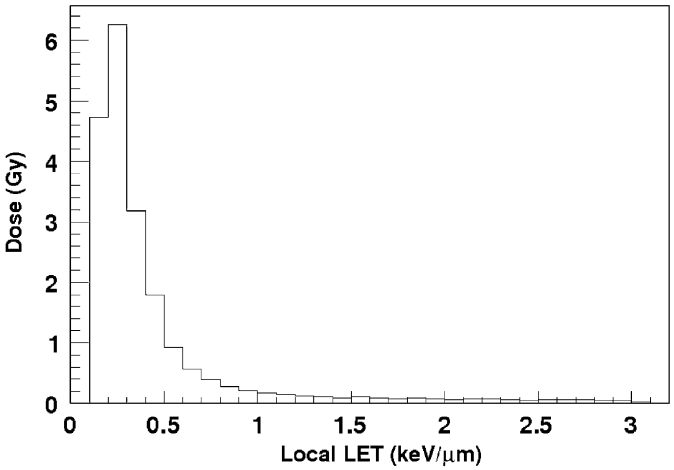

Fig. 3. Distribution of the local LET of particles calculated with the simulation during photon irradiation of a radiochromic film at 20 Gy. Each entry of the histogram is weighted with the dose deposited along the steps.

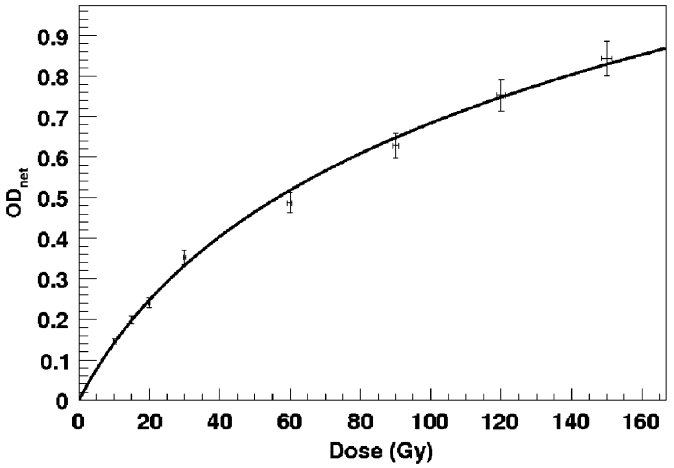

Fig. 4. Measured net optical density of radiochromic film irradiated with photon beam as a function of the dose measured by the ionization chamber (black dots). The error bars indicate the precision of measurements. The black line corresponds to the fitted curve.

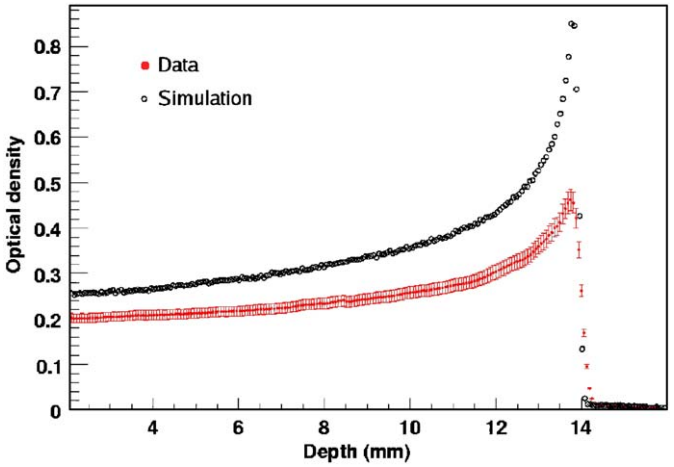

Fig. 5. Measured net optical density of a radiochromic film irradiated at 20 Gy with the ^{13}C beam as a function of the position along the x axis of the film (red dots). The error bars indicate the precision of measurements. Calculated optical density obtained using Eq. (10) with the simulation (black circles). (For interpretation of the references to color in this figure legend, the reader is referred to the web version of this article.)

maximum deposited dose was positioned at 13.7 mm for the ^{13}C beam and at 19.6 mm for the ^{12}C beam.

In Geant4 simulation, the particle tracks are composed of steps. Each step contains all the information about interactions of the particle with matter. To calculate the local LET of the particle, the energy of each particle deposited along the step is divided by the step length. In Geant4 simulation, the energy deposited by a charged particle depends on the electron production threshold. If the range of the secondary particle is below the threshold, the particle is not produced and the energy is deposited continuously along the track of the parent particle. This energy contributes to increasing the local LET of the parent particle. Thus, the choice of the threshold is crucial. The value of the threshold had to be equal or less than the radius r (see Section 2). For this study, the value of the threshold was fixed to 1 μm. In PMMA, the corresponding energy threshold is about 320 eV.

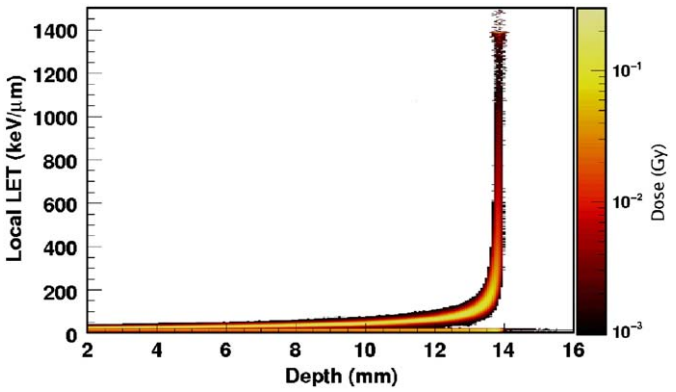

Fig. 6. 2D distribution of the position along the Bragg curve and the local LET in the simulation. Each entry corresponds to a different step of the simulation weighted by the deposited dose at this step.

4. Results

4.1. Photon irradiations

The response of a film irradiated by a photon beam has a weak beam energy dependence [7]. Fig. 3, obtained with the simulation, shows that the local LET of particles was small, with a peak at 0.25 keV/μm. In this case, the optical density was expressed with Eq. (10) and a scale factor k:

$$OD^{net}(D) = k\,\log(a' \cdot D + 1). \tag{16}$$

In our experiment, $k = 1$ but the value of the scale factor k may depend on the type of scanner and softwares used. Films were irradiated at several doses between 0 and 150 Gy. Fig. 4 shows the net optical density as a function of dose. The curve was fitted with Eq. (10) where a' is the free parameter. The value of the fitted parameter a' was 0.0383 Gy^{-1} with an error of 2.7%. Error was estimated with the χ^2 method. Note that the value of the parameter depends on the type of scanner and softwares used. The calibration curve may also vary with the production batch of the film.

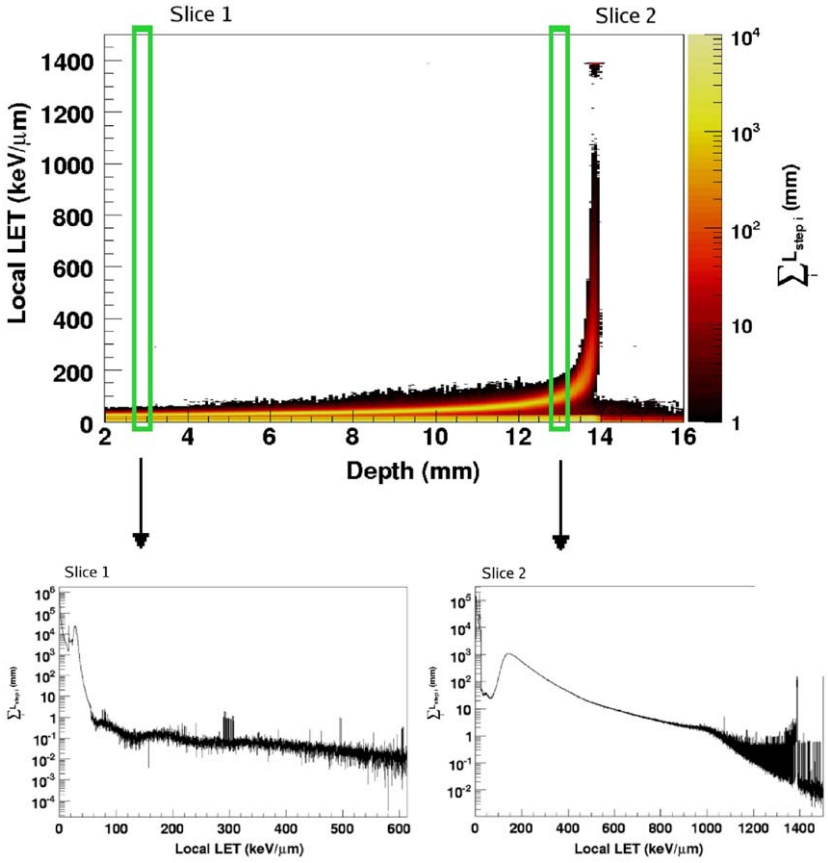

Fig. 7. Top: 2D distribution of the position along the Bragg curve and the local LET in the simulation. Each entry corresponds to a different step of the simulation weighted by step length. Bottom: example of slices at two positions marked by green boxes along the x axis of the 2D distribution. Each slice corresponds to the distribution of the local LET in the simulation. (For interpretation of the references to color in this figure legend, the reader is referred to the web version of this article.)

The approach proposed by Devic et al. [8] gave similar results but they used three free parameters while we had only one parameter and one scale factor in our approach.

4.2. Ion irradiations

We compared the film responses induced by photon beam and ion beam irradiations. We used Eq. (10) to calculate the optical density with the simulation when using a radiochromic film irradiated at 20 Gy with the ^{13}C beam. The result is plotted in Fig. 5. The calculated optical density (black circles) was higher than the measured optical density (red dots) showing that Eq. (10) is not suitable for ion irradiation.

We used the position along the x axis of the film and the local LET of each step calculated in the simulation to generate a 2D histogram. Each entry was weighted by the deposited dose at each step (Fig. 6). The local LET distribution included a low local LET region due to electrons and a high local LET region due to ions. Ion local LET increased in the Bragg peak region. Indeed, the ionization and the fraction of ionization electrons below the production threshold increased along the Bragg curve. In comparison, the local LET for photon irradiation was very low (Fig. 3). With such high local LET particles, it was necessary to apply Eq. (13) to calculate the optical density.

To use Eq. (13), we had to determine the parameter τ. Again, we created a 2D histogram using the position along the x axis of the film and the local LET at each step. But in this histogram, each entry was weighted by the length of the step (see Fig. 7). For a given position x along the Bragg curve, a slice of the histogram (green box) indicates the distribution of the local LET. Each slice allowed to calculate the effective dose at position x with Eq. (12):

$$D_{eff}(x) = \frac{1}{M}\sum_{i=0}^{\#bins} L_i(x)\tau \ln\left(\frac{b_0 + i\cdot b_s}{\tau} + 1\right) \quad (17)$$

where $L_i(x)$ is the sum of step lengths in bin i at a position x along the Bragg curve, b_0 is the center of the first bin and b_s is the bin size. Finally, using Eq. (13), we calculated the optical density and compared this result with the optical density measured at the same position x. We determined τ by fitting the data with Eq. (13) modified with Eq. (17) where τ is the only free parameter. The result for the ^{13}C beam is shown in Fig. 8. The bottom of Fig. 8 is an enlarged view of the Bragg peak area. The value of the fitted parameter τ was 23.82 keV/μm with an error of 1.8% estimated using the χ^2 method. The agreement between the data and the fit was good except after the Bragg peak, as confirmed in Fig. 9. The relative error between the data and the simulation was less than 2%, except immediately before the peak where the error was less than 4%. After the Bragg peak, the calculated optical density decreased faster than the measured optical density. This difference is more visible on the enlarged view. The difference at the end of the peak reached 0.2 mm.

We used the fitted τ to calculate the optical density for the ^{12}C beam directly in the simulation. The result is shown in Fig. 10. The agreement between the data and the simulation was good. The relative error between data and simulation was less than 2% except in the region around 16 mm where the error was less than 5%. We also determined τ by fitting the ^{12}C data. The value of the fitted parameter τ was 24.37 keV/μm with an error of 1.6%. After the Bragg peak, we observe the same slope difference than in the previous section. One explanation could be the limit of the Geant4 physic models when used at low energy. Indeed, Geant4 tends to underestimate the tail dose coming from the beam fragmentation. This difference was consistent with the results of Pshenichnov et al. [9]. An other explanation could be an energy diffusion along polymer chains.

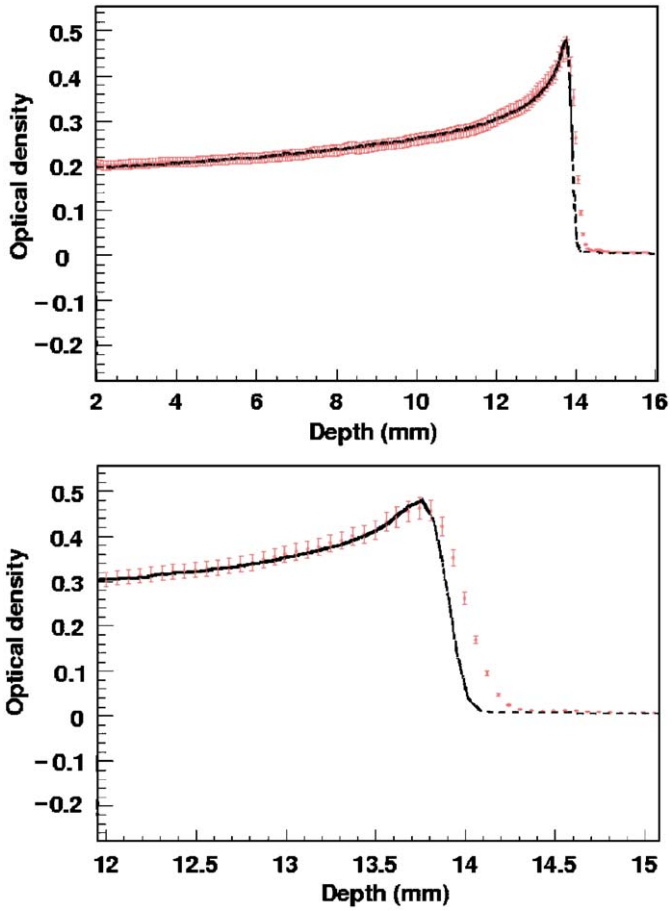

Fig. 8. Top: measured net optical density of a radiochromic film irradiated at 20 Gy with the ^{13}C beam as a function of the position along the x axis of the film (red dots). Error bars indicate the precision of measurements. The black dotted line is the fitted curve obtained with Eq. (13). Bottom: enlarge view of the Bragg peak (between 12 and 15 mm). (For interpretation of the references to color in this figure legend, the reader is referred to the web version of this article.)

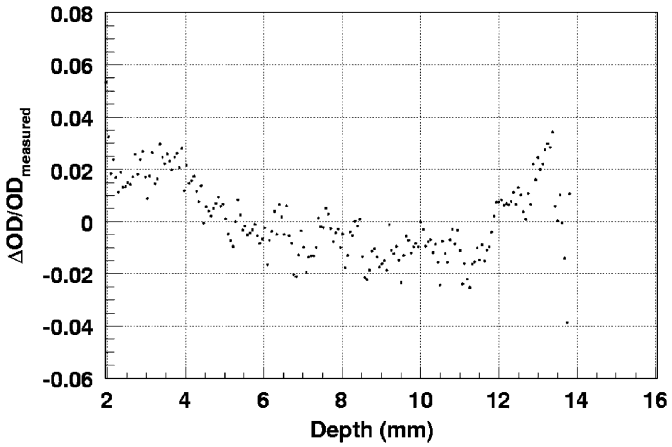

Fig. 9. Relative difference between measured and simulated net optical density of a radiochromic film irradiated at 20 Gy with the ^{13}C beam as a function of the position along the x axis of the film. The scale of the y axis is set between −0.06 and 0.08.

In our experiments, the optical density calculated with the simulation gave the same result as the fitted curve. If future measurements with other beam types confirm the present conclusions, the fitted should be used to calculate the optical

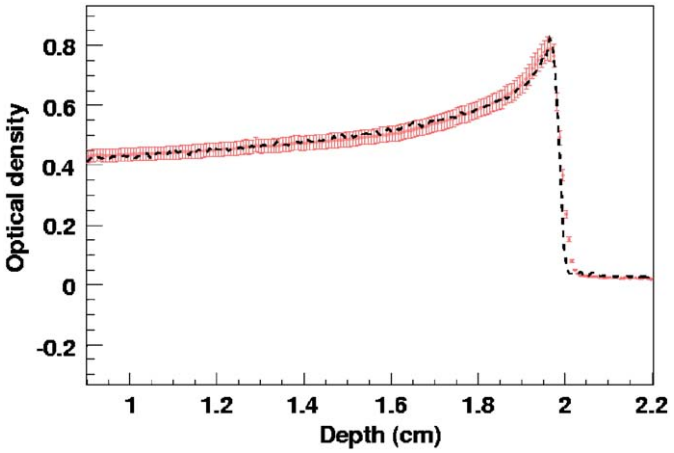

Fig. 10. Measured net optical density of a radiochromic film irradiated at 60 Gy with the ^{12}C beam as a function of the position along the x axis of the film (red dots). Error bars indicate the precision of measurements. The black dotted line is the optical density calculated directly in the simulation with the τ fitted on the ^{13}C data. (For interpretation of the references to color in this figure legend, the reader is referred to the web version of this article.)

density directly in the simulation for any beam type including complex multibeam configuration.

5. Conclusion

From the study of the film irradiated with photons, we generated a calibration curve which allowed to determine the radiation dose from optical density measurements. We determined the main parameter α' involved in film response. This parameter is dependent on the characteristics of the scanner and the softwares used for the analysis. We have developed a model which allows to calculate the response of the film to ion irradiation in the simulation. This model is based on the response of the film to photon irradiation and its saturation by high local energy deposition computed by Monte-Carlo simulation. The cylinder used for the calculation of the local LET is chosen smaller than the size of polymer microcrystals, and thus the cut parameters must be set accordingly. The first results show good agreement between measurement and simulation. The significant improvement achieved with the implementation of the model is pointed out by the comparison between Figs. 5 and 8. In the energy range of our applications, the slope difference after the Bragg peak is small. We were especially interested in the first part of the Bragg curve, however, we will continue to study the film response to investigate this difference. We have to test our model with more experiments with various beam types (different types of particles and different energies) to verify that all parameters are well taken into account. We will also try to enhance our model to improve its accuracy. The first tests were realized with a beam of ^{13}C and a beam of ^{12}C. In a second step, we plan to perform other experiments with proton irradiation and ^{12}C beam to operate in the conditions of medical hadrontherapy.

Acknowledgments

Our work is funded by the French National Research Agency: SIMCA2 Project (ANR-06-BLAN-0125) and fGATE project (ANR-06-CIS-004). We thank the C. Rodriguez's team, M. Bajard and the CIRIL for the technical support.

References

[1] Radiation Therapy Committee Task Group No. 55, Radiochromic film dosimetry, AAPM Report No. 63, 1998.
[2] W. McLaughlin, M. Al-Sheikhly, D. Lewis, A. Kovács, L. Wojnárovits, Radiochromic solid-state polymerisation reaction, Irradiation of Polymers Fundamentals and Technological Applications, 1996, pp. 152–166.
[3] M.J. Butson, P.K.N. Yu, T. Cheung, P. Metcalfe, Mater. Sci. Eng. R 41 (2003) 61.
[4] L.E. Reinstein, G.R. Gluckman, H.I. Amols, Med. Phys. 24 (12) (1997) 1935.
[5] S. Jan, et al., Phys. Med. Biol. 49 (2004) 4543.
[6] S. Agostinelli, et al., Nucl. Instr. and Meth. A 506 (2003) 250.
[7] M.J. Butson, T. Cheung, P.K. Yu, Appl. Radiat. Isot. 64 (1) (2006) 60.
[8] S. Devic, J. Seuntjens, E. Sham, E.B. Podgorsak, C.R. Schmidtlein, A.S. Kirov, C.G. Soares, Med. Phys. 32 (7) (2005) 2245.
[9] I. Pshenichnov, I. Mishustin, W. Greiner, Neutrons from fragmentation of light nuclei in tissue-like media: a study with geant4 toolkit, 2005.